Compressive sensing framework for time-lapse seismic data reconstruction using the linear Radon transform

Pedro C. de Assis*, Romulo B. da Silva, Alan C. Galante, and Irineu A. Lima Neto, FACC Foundation; Roseane M. Missagia, and Marco A. R. Ceia, North Fluminense State University (UENF), and INCT-Geofísica

Abstract

This work shows how the ideas of the Compressive Sensing (CS) theory help us create economic time-lapse seismic acquisitions by randomly allocating a smaller number of sources and/or receivers and relaxing the survey replication. The framework was applied to synthetic 2D time-lapse data that mimics a marine seismic acquisition. We modeled two subsampled surveys, named as baseline and monitor by removing 50% of the shot families and applied a sparsity-promoting program to recover the datasets in the original grid. The results showed that we can achieve high-quality pre-stack data after recovery, even considering a smaller number of records in a regular grid, demonstrating that CS ideas could be successfully applied to recover missing data.

Introduction

The reservoir characterization and monitoring is a continuous process that involves the acquisition, processing, and integration of geophysical data aimed to obtain properties of formations and evaluate the behavior of the reservoir. The time-lapse seismic plays a key role in this process in evaluating the reservoir properties and fluid saturation changes along with time in areas not sampled by wells.

The time-lapse monitoring is characterized by an initial seismic acquisition, called baseline, and later ones are called monitor, which aims to repeat, as much as possible, the previous survey design (Oghenekohwo et al., 2014). To ensure the repeatability between seismic surveys the companies deal with environmental and operational challenges, such as tidal differences, infrastructure in the survey area, etc. According to Lecerf & Reiser (2004), the seismic data resolution must also be high enough to image small property changes within a layer, so it becomes necessary to acquire densely sampled seismic data.

The high costs associated with time-lapse monitoring led to the development of seismic acquisition designs based on Compressive Sensing (CS) ideas (Donoho, 2006; Candes & Tao, 2006), which were initially proposed in the works of Hennenfent & Herrmann (2008), Herrmann (2010), and Mansour et al. (2012). The advantages of randomly subsampled acquisitions, the reduction of acquisition time, and also the operational costs were extended to time-lapse acquisitions in the work of Oghenekohwo et al. (2014) considering the non-repeatability of surveys.

Since the baseline and the monitor share information, especially when analyzed in a sparse domain, Oghenekohwo et al. (2014) proposed a Joint Recovery Model (JRM), which exploits the advantages of the Distributed Compressive Sensing (DCS), proposed by Baron et al. (2009), where the inversion problem considers the common information between the baseline and the monitor to recover the densely sampled time-lapse data. The JRM has demonstrated better recovery results compared to the Independent Recovery Strategy (IRS), which applies a standard recovery for each survey (Oghenekohwo et al., 2017).

The data reconstruction can also be improved by choosing an appropriate sparsifying transform during the CS recovery process (Herrmann, 2010). As well as other sparsifying transforms, e.g., Wavelet and Curvelet, the linear Radon (tau-p) transform can attain high compression rates of seismic data based on data summation over straight lines with the integration paths constrained by the ray parameters (Aharchaou & Levander, 2016).

In this work, we evaluate the potential of the CS in the reconstruction of synthetic time-lapse seismic data using the JRM and IRS methods. The study focused on the impact of replicated and non-replicated randomized surveys on increasing the recovered data quality and efficiency of signal processing, highlighting the potential for further application in the field. We also exploited the key components stated by CS theory: a sparsifying signal representation using the linear Radon transform, a randomized seismic acquisition, and a sparse recovery by one-norm minimization.

Compressive Sensing

The CS reconstruction scheme for regularly sampled datasets with traces missing follows the forward model,

$$y = RS^H x, \tag{1}$$

here $y \in \mathbb{R}^n$ represents the acquired data with incomplete measurements, $R \in \mathbb{R}^{nxN}$ with $N \gg n$ the restriction operator, which maps the positions with missing data, and $S^H \in \mathbb{C}^{NxP}$ with $P \geq N$ the adjoint operator of the sparsifying transform, responsible to convert the data in some sparse domain into the time-space domain. $x \in \mathbb{C}^P$ is the sparse representation of the complete dataset $d \in \mathbb{R}^N$.

We can recover x by solving the following sparsity-promoting convex optimization program for noise-free data,

$$\tilde{x} = argmin_x \|x\|_1 \ s.t. \ y = RS^H x. \quad (2)$$

The solution of the optimization problem gives the sparsity vector $\tilde{x}$ that has the smallest one-norm subject to fitting the observed data. To arrive at this solution, we use the software SPGl1 (Van Den Berg & Friedlander, 2009). The recovered sparsity vector $\tilde{x}$ gives the reconstructed data $\tilde{d} = S^H \tilde{x}$.

The operator S^H was built by considering the adjoint operator of the chirp Radon transform (Andersson & Robertsson, 2019), which is more straightforward and faster than the standard linear Radon transform. Its linear operator is available in the package PyLops (Ravasi & Vasconcelos, 2020).

Independent Recovery Strategy (IRS)

The IRS for time-lapse data applies the CS formulation to recover independently the randomly subsampled surveys of the baseline and monitor as

$$y_i = R_i S_i^H x_i, \ for \ i \in \{1,2\}, \quad (3)$$

here, the subscript i represents the incomplete surveys for the baseline (1) and the monitor (2). The sizes of the subsampled surveys do not need to be necessarily equal, as well as the recovery grid. Respecting the key ideas of CS we can recover each survey by solving the eq. 2. The time-lapse signal is obtained by subtracting the recovered surveys.

Joint Recovery Method (JRM)

The JRM proposed by Oghenekohwo et al. (2014) performs a joint inversion by taking into account the shared information between the baseline and monitor surveys. The recovery problem involves the system of equations,

$$\begin{bmatrix} y_1 \\ y_2 \end{bmatrix} = \begin{bmatrix} A_1 & A_1 & 0 \\ A_2 & 0 & A_2 \end{bmatrix} \begin{bmatrix} z_0 \\ z_1 \\ z_2 \end{bmatrix} \approx y = Az, \quad (4)$$

here $A_i = R_i S_i^H$ with the subscript i representing the survey index. The sparsity-promoting program recovers z by solving $\tilde{z} = argmin_z \|z\|_1 \ s.t. \ y = Az.$, which is a vector composed of the common component between the surveys z_0 and the innovations for the baseline and the monitor with respect to the common component $z_i \ for \ i \in \{1,2\}$. The estimated sparse representations of the surveys $\tilde{x}_i$ are given by

$$\tilde{x}_i = \tilde{z}_0 + \tilde{z}_i, \quad (5)$$

which give the reconstructed data $\tilde{d}_i = S_i^H \tilde{x}_i$ for the baseline ($\tilde{d}_1$) and monitor ($\tilde{d}_2$). The time-lapse data is contained in the difference between the innovations $\tilde{z}_1$ and $\tilde{z}_2$.

Numerical Results

This section shows the results of the IRS and JRM methods in the recovery of synthetic 2D time-lapse seismic data generated from a realistic velocity model of a petroleum system. From a noise-free case, we analyzed the influence of the degree of repeatability between baseline and monitor surveys during the application of the recovery methods under study. The time-lapse seismic data is available from the SINBAD consortium (ftp://ftp.slim.gatech.edu/data/SoftwareRelease/Acquisition/TimeLapseJRM/data). The baseline data was modeled from an initial velocity model, while the monitor data was acquired after a fluid substitution in a section of the reservoir.

The modeling of each dataset was carried out from a conventional geometry, considering spatial sampling of 12.5 m for sources and receivers. The baseline and monitor datasets have 512 time samples, 151 receivers, 151 sources, and a sampling rate of 4 ms. The seismic data modeling did not include noise, so the difference between the two surveys represents only the time-lapse data, which has a low amplitude (about 10%) when compared to the surveys amplitudes (Oghenekohwo, 2017). Figure 1 shows the baseline, monitor, and time-lapse original common receiver gathers, containing the 151 shot positions. The fluid substitution led to changes in signal amplitudes recorded near the reservoir.

The subsampling of the surveys was performed in the source domain to represent a marine streamer survey with a smaller number of shots deployed to apply our CS framework. Considering the original data with 151 shots points, we removed 50% of the shot gathers to obtain the subsampled data. Figure 2 displays the source positions of the subsampled data. Those source coordinates were obtained from modeling an optimized subsampled acquisition geometry considering the maximum gap size control of 4 sources.

This study also analyzed the impact of repeatability between baseline and monitor shot positions during recovery. After fixing the subsampled baseline survey, 2 monitor subsampled surveys were modeled with different overlap percentages about the baseline survey: 30%, and 100%. The 30% overlap indicates that only 30% of the trace positions present in the monitor gather are also present in the baseline gather, while the 100% overlap indicates that all trace positions are common for them. Since the survey geometry is split-spread, we conducted the recovery by using the 2D chirp Radon operator with ray parameters px ranging between $\pm$ 0.0012. The sparse optimization problem was solved using the package SPGL1 using 400 iterations.

The IRS and JRM approaches were applied to the subsampled common receiver gathers and considered the repeatability analysis described above. Figure 3 displays the IRS results from the monitor gather according to the repeatability of the surveys. The recovery provided high-quality data with good trace amplitude, wavefront continuity, and low noise levels. This behavior occurs at all degrees of repeatability (gathers in Figure 3-a,b). The residuals

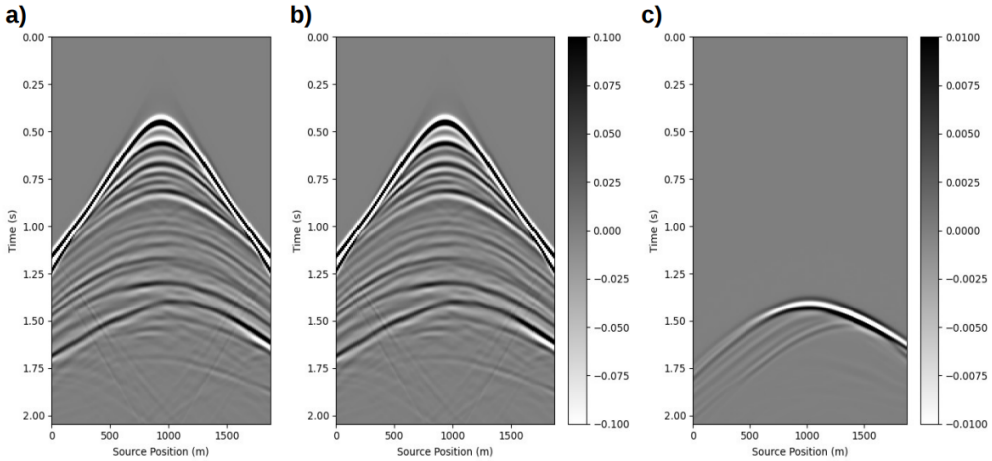

Figure 1 – The original common receiver gathers from the (a) baseline, (b) monitor, and (c) time-lapse difference. Due to the low amplitude of the time-lapse data, its color scale is one-tenth the scale of the baseline and monitor data.

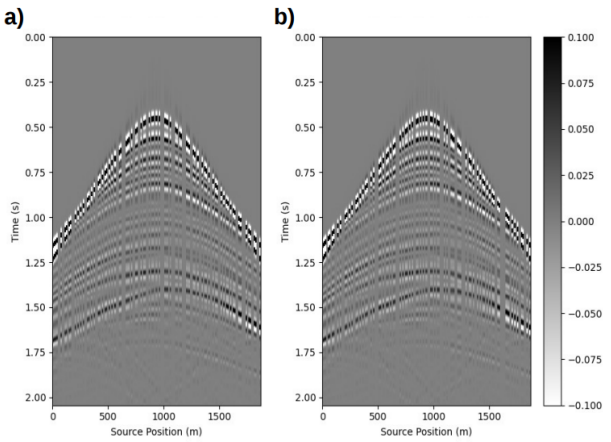

Figure 2 – Common receiver gathers of subsampled acquisitions from (a) baseline, and (b) monitor. The random subsampling method takes into account a maximum gap of 4 missing sources.

of the estimations are shown by the gathers in Figure 3-c,d. Analyzing the Signal-to-Noise Ratio (SNR) in Table 1, the performance of the IRS method does not depend on the percentage of repeatability between surveys due to the independent recovery process. Only parameters linked to the acquisition geometry, such as the subsampling ratio and the occurrence of wide gaps without traces, could affect data recovery with this method. The baseline results are not shown as they are similar to the monitor data.

The IRS results for the time-lapse data are shown in Figure 4-a,b for the different repeatability values. The data recovered with 30% repeatability showed a high level of noise with a low SNR of -11.2 dB (Table 1). The gather with 100% repeatability presented a better result estimating only the amplitude referring to the time-lapse difference, with SNR of 8.6 dB (Table 1). The gathers in Figure 4-c,d represent the residuals of the estimates. Due to the recovery to insert some noise in the baseline and monitor

Table 1 – The SNR values (dB) of the recovered gathers from baseline, monitor, and time-lapse via JRM and IRS methods for 30%, and 100% repeatability between surveys.

Overlap	**Baseline**		**Monitor**		**Time-lapse**	
	JRM	IRS	JRM	IRS	JRM	IRS
30%	28.0	21.3	28.1	21.3	2.6	-11.2
100%	21.3	21.3	21.3	21.2	21.2	8.6

gathers, the time-lapse data also presents noise. This behavior is more evident in the case of 30% repeatability. For recovery with 100% repeatability, the fact that the positions without traces are the same for the baseline and monitor leads to the partial suppression of noise inserted during recovery, improving the SNR. This indicates the presence of coherent noise between the two recovered gathers when the A_1 and A_2 matrices are equal.

The JRM results for the monitor gather for the different repeatability degrees are shown in Figure 5-a,b, with the residuals in Figure 5-c,d. As for the IRS approach, the recovered monitor gathers show high resolution, continuity of reflections, and low noise levels at all repeatability levels. Analyzing the SNR values in Table 1, the JRM approach performs better than the IRS, which is explained by the jointly sparse inversion process that exploits the shared information between the surveys. The SNR value also decreases with increasing repeatability. For 30% repeatability, there is better wavefield coverage (sampling), and the baseline information contributes to recovering the missing information in the monitor survey (and vice versa). For 100% repeatability, the reduction of the wavefield sampling leads to a lower quality of the recovered surveys.

The JRM results for the time-lapse data are shown in Figure 6-a,b, which are less noisy compared to the IRS approach. The recovered time-lapse data has also good resolution and continuity, although the gather with 30% overlap (Figure 6-a) has higher noise levels, especially at

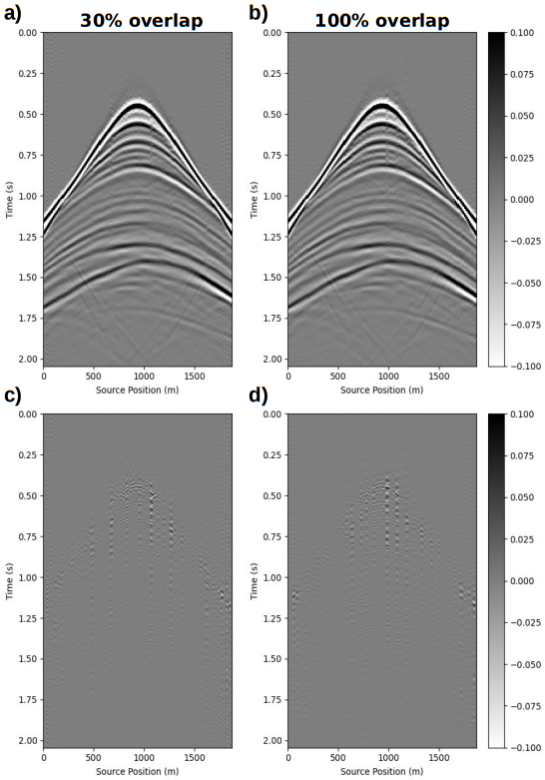

Figure 3 – The gathers recovered via IRS from the monitor survey with (a) 30%, and (b) 100% overlap. (c,d) The corresponding residuals from the original gather.

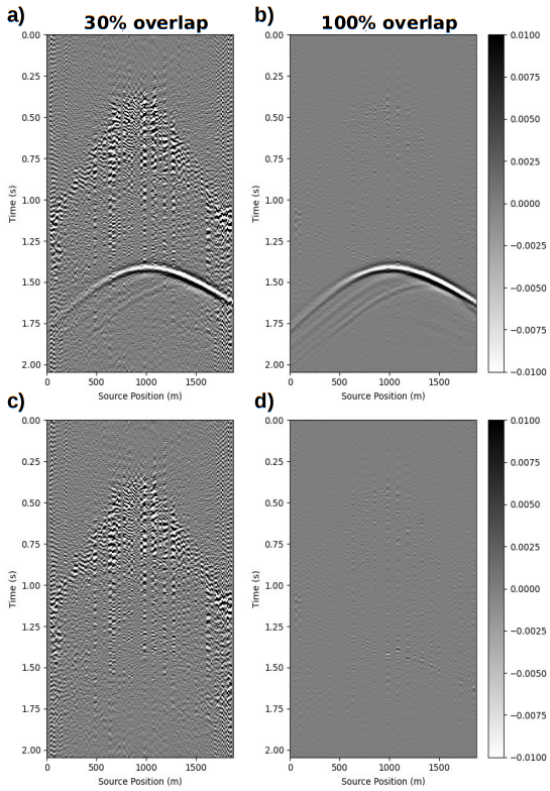

Figure 4 – The gathers recovered via IRS from the time-lapse data with (a) 30%, and (b) 100% overlap. (c,d) The corresponding residuals from the original gather.

the edges. The gather with 100% repeatability (Figure 6-b) showed significant improvements during recovery. The gathers in Figure 6-c,d represent the residuals of these estimates. From the SNR values in Table 1, the JRM method has a better performance than IRS at all repeatability degrees, although it presents a higher computational cost due to joint inversion. Due to the recovery errors in the surveys gathers, the time-lapse difference is also contaminated by noise. This behavior is highlighted in the result with 30% repeatability. For the recovery with 100% repeatability, the noise in the recovered gathers are practically eliminated during the time-lapse difference since the positions with missing traces are the same for both surveys. This behavior indicates the presence of a coherent noise between the two gathers, when the matrices A_1 and A_2 are equal.

Conclusion

The ideas of CS provide a new model for time-lapse seismic data acquisition that reduces the survey costs while keeping the data resolution. The main advantages are related to the survey time reduction due to the smaller amount of data to be acquired and the possibility of relaxing the need for seismic surveys with high repeatability. We showed how the recovery could be improved by using a correct random subsampling scheme, a sparsifying transform that effectively matches the observed data, and approaches that exploit the shared information between the surveys. The recovered baseline, monitor, and time-lapse gathers showed high-quality data with lower noise levels and better continuity of the wavefronts when using the JRM approach. Those results supply that CS ideas can be successfully applied to obtain high-resolution time-lapse images after processing data with fewer measurements.

Acknowledgments

Authors thanks UENF/LENEP for all structure provided to the execution of this work. We also would like to thank the authors of PyLops (https://github.com/PyLops/pylops) and SPGL1 (https://friedlander.io/spgl1). This study was financed in part by the CAPES/Brazil; Petrobras (Process 2017/00067-9). RM and MC thank INCT-Geofísica for financial support; and CNPq for their Research Grants of Productivity in Technological Development and Innovation – DT II (313746/2019-2 and 313522/2019-7).

References

Aharchaou, M. & Levander, A., 2016. A compressive sensing approach to the high-resolution linear radon transform: application on teleseismic wavefields, Geophysical Supplements to the Monthly Notices of the Royal Astronomical Society, vol. 207(2): 811–822.

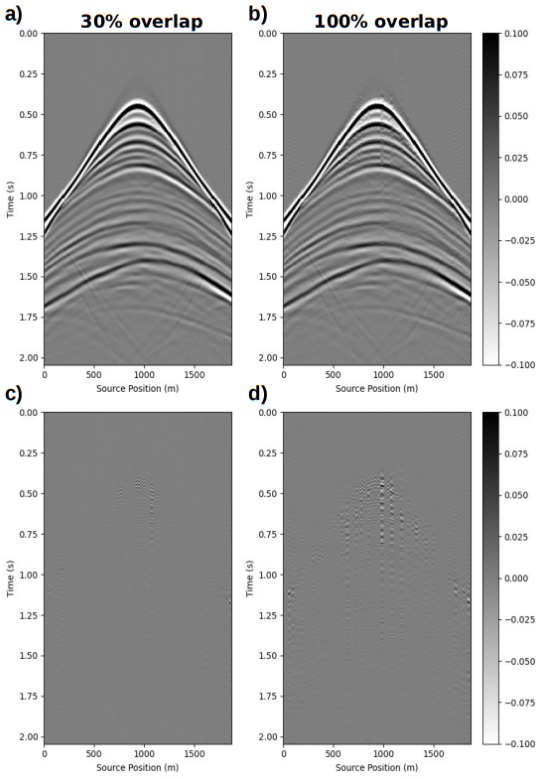

Figure 5 – The gathers recovered via JRM from the monitor survey with (a) 30%, and (b) 100% overlap. (c,d) The corresponding residuals from the original gather.

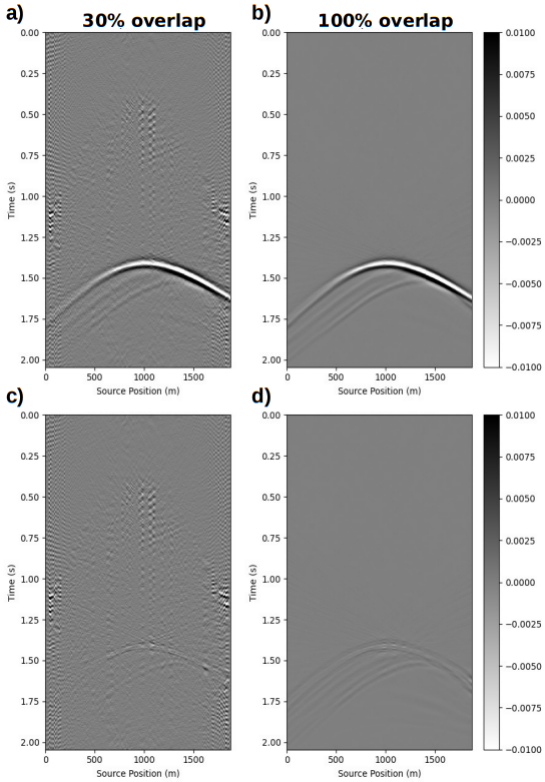

Figure 6 – The gathers recovered via JRM from the time-lapse data with (a) 30%, and (b) 100% overlap. (c,d) The corresponding residuals from the original gather.

Andersson, F. & Robertsson, J., 2019. Fast τ-p transforms by chirp modulation, Geophysics, vol. 84(1): A13–A17.

Baron, D., Duarte, M. F., Wakin, M. B., Sarvotham, S. & Baraniuk, R. G., 2009. Distributed compressive sensing, doi:DOI:10.21236/ada521228.

Candes, E. J. & Tao, T., 2006. Near-optimal signal recovery from random projections: Universal encoding strategies, IEEE Transactions on Information Theory, vol. 52(12): 5406–5425, doi:10.1109/tit.2006.885507.

Donoho, D., 2006. Compressed sensing, IEEE Transactions on Information Theory, vol. 52(4): 1289–1306, doi:10.1109/TIT.2006.871582.

Hennenfent, G. & Herrmann, F. J., 2008. Simply denoise: Wavefield reconstruction via jittered undersampling, GEOPHYSICS, vol. 73(3): V19–V28, doi:https://doi.org/10.1190/1.2841038.

Herrmann, F. J., 2010. Randomized sampling and sparsity: Getting more information from fewer samples, GEOPHYSICS, vol. 75(6): WB173–WB187, doi: https://doi.org/10.1190/1.3506147.

Lecerf, D. & Reiser, C., 2004. High-resolution processing for time-lapse seismic, First Break, vol. 22, doi: https://doi.org/0.3997/1365-2397.22.8.25983.

Mansour, H., Wason, H., Lin, T. T. & Herrmann, F. J., 2012. Randomized marine acquisition with compressive sampling matrices, Geophysical Prospecting, vol. 60(4): 648–662, doi:https://doi.org/10.1111/j.1365-2478.2012.01075.x.

Oghenekohwo, F., 2017. Economic time-lapse seismic acquisition and imaging -Reaping the benefits of randomized sampling with distributed compressive sensing, Ph.D. Thesis, The University of British Columbia.

Oghenekohwo, F., Esser, E. & Herrmann, F., 2014. Time-lapse seismic without repetition - reaping the benefits from randomized sampling and joint recovery, Conference Proceedings, 76th EAGE Conference and Exhibition 2014: 1–5, doi:https://doi.org/10.3997/2214-4609.20141478.

Oghenekohwo, F., Wason, H., Esser, E. & Herrmann, F. J., 2017. Low-cost time-lapse seismic with distributed compressive sensing - part 1: Exploiting common information among the vintages, GEOPHYSICS, vol. 82(3): P1–P13.

Ravasi, M. & Vasconcelos, I., 2020. Pylops - a linear-operator python library for scalable algebra and optimization, SoftwareX, vol. 11: 100361.

Van Den Berg, E. & Friedlander, M. P., 2009. Probing the pareto frontier for basis pursuit solutions, SIAM Journal on Scientific Computing, vol. 31(2): 890–912.